
WHO EXPLAINS THE EXPLANATION? QUANTITATIVELY ASSESSING FEATURE ATTRIBUTION METHODS

A PREPRINT

 **Anna Arias-Duart**

Barcelona Supercomputing Center (BSC)
anna.ariasduart@bsc.es

 **Ferran Parés**

Barcelona Supercomputing Center (BSC)
ferran.pares@bsc.es

 **Dario Garcia-Gasulla**

Barcelona Supercomputing Center (BSC)
dario.garcia@bsc.es

ABSTRACT

AI explainability seeks to increase the transparency of models, making them more trustworthy in the process. The need for transparency has been recently motivated by the emergence of deep learning models, which are particularly obscure by nature. Even in the domain of images, where deep learning has succeeded the most, explainability is still poorly assessed. Multiple feature attribution methods have been proposed in the literature with the purpose of explaining a DL model’s behavior using visual queues, but no standardized metrics to assess or select these methods exist. In this paper we propose a novel evaluation metric — the *Focus* — designed to quantify the faithfulness of explanations provided by feature attribution methods, such as LRP or GradCAM. First, we show the robustness of the metric through randomization experiments, and then use *Focus* to evaluate and compare three popular explainability techniques using multiple architectures and datasets. Our results find LRP and GradCAM to be consistent and reliable, the former being more accurate for high performing models, while the latter remains most competitive even when applied to poorly performing models. Finally, we identify a strong relation between *Focus* and factors like model architecture and task, unveiling a new unsupervised approach for the assessment of models.

1 Introduction

Explainability has become a major topic of research in Artificial Intelligence (AI), aimed at increasing trust in models such as Deep Learning (DL) networks. However, trustworthy models cannot be achieved with explainable AI (XAI) methods unless the XAI methods themselves can be trusted.

Most evaluation on XAI methods measure their interpretability, which qualitatively measures how understandable an explanation is to humans Gilpin et al. [2018]. While interpretability is essential for humans to interact with the model, its evaluation generally involves end-users in the process Mohseni et al. [2018], inducing strong biases. Furthermore, for enabling trust on XAI methods and their explanations, a qualitative evaluation alone does not guarantee coherency to reality (*i.e.*, model behavior). To that end, quantitative and objective evaluations are needed.

The challenge of quantitatively evaluating XAI methods lies in the absence of a ground truth: we cannot be sure of what a DL method is or should be doing. Nonetheless, we wish our XAI methods to be consistent, as a true but incomprehensible explanation is preferable to a false one. This can be achieved by evaluating the faithfulness Selvaraju et al. [2019] of the explanation *w.r.t.* the underlying model, discerning between accurate and misleading explanations. In this paper we propose a novel methodology for that purpose, demonstrating its use on the evaluation of *feature attribution* methods when applied on models trained for image classification. These methods try to approximate the contribution of pixels to the output, like the gradient method Simonyan et al. [2014], Smoothgrad Smilkov et al. [2017], Layer-wise Relevance Propagation (LRP) Bach et al. [2015] or GradCAM Selvaraju et al. [2019].

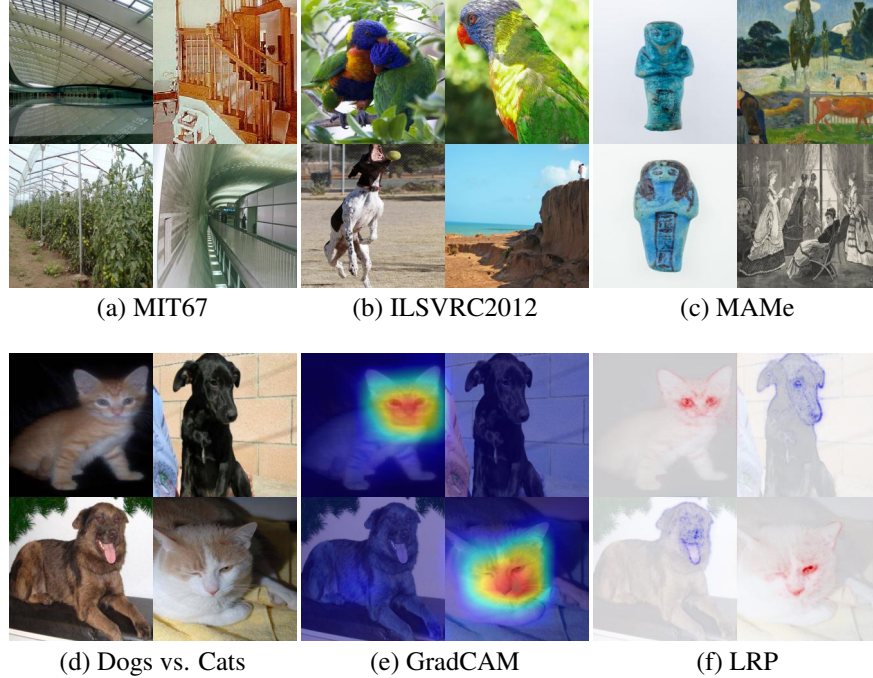


Figure 1: First row: Sample of mosaics used by the evaluation methodology, obtained for: (a) MIT67 (b) ImageNet (ILSVRC2012) (c) MAMe. Second row: example of input mosaic from Dogs vs. Cats (d), and the explanations obtained by GradCAM (e) and LRP (f) for the target class *cat*.

To further motivate our work, let us discuss the limitations of single-sample assessment. When a unique instance is processed by a XAI method, the explanations generated are specific to that instance and its associated label, the whole process lacking sources of noise. In this context it is impossible to assess faithfulness, since, even explanations which seem inappropriate (*e.g.*, the background of the image instead of the central object) may be accurate to the model’s behavior following a bias learnt by the model. This paper introduces a problem for XAI methods in which they may objectively err (*i.e.*, focus on something the model is not focusing on), as means to approximate faithfulness. In the context of image deep learning, we do so by creating an image composed of samples of different classes (named the *mosaic image*) and asking a XAI method to provide explanation for just one of those classes. In a sort of eye-tracking game, we measure how much of the explanation generated by the XAI method is located on the parts of the mosaic corresponding to the target class, and quantify it through the *Focus* metric.

We perform a set of experiments to evaluate the consistency and robustness of the *Focus* metric on various XAI methods, network architectures and datasets. We start by computing the *Focus* metric on models with random weights, as generating good explanations in arbitrary models is a known weakness of XAI methods Adebayo et al. [2018]. Having assessed that a random model has a random *Focus*, we consider the relation between model performance and *Focus* score. While better performing models yield better *Focus* overall (with Pearson correlations above 0.98), we also find *Focus* to be related with factors such as the architectures or the target task. These results suggest the *Focus* provides additional information on model behavior, beyond what is typically assessed by performance metrics, pointing towards its potential use in model selection. In the end, we find the proposed *Focus* metric to be a good approximation to faithfulness, particularly within the challenging context of DL.

2 Related Work

The lack of a ground truth to compare against has resulted in a wide variety of quantitative measures targeting the evaluation of *feature attribution* methods. The ones introduced in Bach et al. [2015] highlight *Explanation Continuity* and *Explanation Selectivity*. The first measures function continuity following the idea that similar inputs (images) should produce similar outputs (explanations). That is quantified by calculating the maximum variation of the explanation *w.r.t.* input variation. The second property checks if pixels are relevant for the model’s prediction by checking the effect of removing them. This is related with the *pixel flipping* algorithm Bach et al. [2015], which performs a semi-quantitative

analysis by perturbing pixels from patches with the greatest relevance, and then assessing the impact on the prediction score.

The authors of Sundararajan et al. [2017] proposed two axioms that XAI methods should satisfy: *Sensitivity* and *Implementation invariance*. The former checks that irrelevant features have no explanation attributed, while the latter checks that functionally similar models produce equivalent attributions. In another work Adebayo et al. [2018] two types of tests are proposed: the *model parameter randomization* test and the *data randomization* test. The first aims to prove that if an explanation depends on the model, a randomized model should produce a different explanation. The second test checks if there exists a relation between the explanation and the labels, that is, if a regular dataset produces different results than one with randomly permuted labels.

Other studies base their evaluation on the premise that relevance should be concentrated on the central object of the target class. In Zhang et al. [2018], authors introduce the *pointing game* technique to evaluate if the point of maximum relevance lies on the object of the target class. Authors also evaluate the localization capacity of methods by drawing bounding boxes from the explanation heatmap and calculating the error *w.r.t.* the correct bounding box Selvaraju et al. [2019]. However, as pointed out by different works Sundararajan et al. [2017], Samek and Müller [2019], the premise that objects are the only important feature for the prediction is false. Finally, Samek et al. [2016] consider the premise that smaller explanations are better, under the assumption that this reduces noise in the generated explanations.

Noticeably, most of these properties, metrics and tests are based on assumptions induced by the human understanding of perception. They are consequences of implicit human cognitive biases. And we cannot be certain that such biases are, or should be aligned with the learning paradigm of DL. Thus, we consider these methods to assess *interpretability* at a certain level. On the other hand, the methods which minimize human bias and approximate *faithfulness* the most are *pixel flipping*, *sensitivity* and *model parameter randomization*. We found these to be closest to our work.

3 Methodology

In this section we define a novel metric — the *Focus* metric —, originally intended to assess the faithfulness of explanations produced by *feature attribution* methods. This score involves three elements: an explainability method (§3.1), a trained model (§3.2), and a set of mosaic samples (§3.3). In the following subsections we discuss these in detail, before defining the *Focus* metric itself (§3.4).

3.1 Explainability methods

Throughout the paper we use and evaluate three *feature attribution* methods:

- Layer-wise Relevance Propagation (LRP) Bach et al. [2015], based on the implementation of Nam *et al.* Nam et al. [2019]. On the first layer use the z^B -rule Montavon et al. [2017], on fully connected layers the LRP- ϵ Bach et al. [2015], and on convolutional layers the LRP- $\alpha\beta$ Bach et al. [2015] with $\alpha = 1$ and $\beta = 0$.
- Gradient-weighted Class Activation Mapping (GradCAM) Selvaraju et al. [2019], based on the implementation of Gildenblat *et al.*¹. We compute the gradients of the logits of the class *w.r.t.* the feature maps of the final convolutional layer. That is, the 5th layer for AlexNet, the 13th for VGG16 and the last layer from the 5th block for ResNet18 (also known as block E).
- SmoothGrad Smilkov et al. [2017], based on the implementation of Nakashima *et al.*². Explanations are obtained computing the gradient of the specific class score *w.r.t.* the input pixels and adding small perturbations on the input image (in our case Gaussian Noise).

3.2 Training set up

To run a XAI method one needs a model to explain. One generated from an architecture trained on a dataset through a specific training configuration. In our experiments, we use the following:

- **Architectures:** AlexNet Krizhevsky et al. [2012], VGG16 Simonyan and Zisserman [2014] and ResNet18 He et al. [2016].
- **Datasets:** the Dogs vs. Cats³, ILSVRC 2012 Russakovsky et al. [2015] (hereafter ImageNet), MIT67 Quattoni and Torralba [2009] and the Museum Artworks Medium dataset (MAMe) Parés et al. [2021].

¹<https://github.com/jacobgil/pytorch-grad-cam>

²<https://github.com/kazuto1011/grad-cam-pytorch>

³<https://www.kaggle.com/c/dogs-vs-cats/overview>

- **Training configurations:** Data augmentation is performed during training: resize to (0.875 x width, 0.875 x height), random rotation from -30 to 30, random crop of (width, height) and horizontal flip with a 50% chance. The terms height and width refer to the input size required by the architecture, 224x224 in the case of AlexNet, VGG16 and ResNet18. As an optimization method we use AMSGrad Reddi et al. [2019]. The training optimization parameters, together with the rest of the code needed to replicate the experiments of this paper can be found in ⁴.

3.3 Mosaic construction

The last element required to compute the *Focus* metric is the mosaic, an image composed by four different samples disposed in a two by two grid. Samples from the training set are never used for mosaics.

To formalize mosaics, and later *Focus*, let us define a dataset D composed by a set of images $I = \{img_1, img_2, \dots, img_n\}$ and a set of classes $C = \{c_1, c_2, \dots, c_k\}$, where n is the number of total images and k is the number of total classes. Every image in I has assigned a unique class from C . From here we build a set of mosaics $M = \{m_1, m_2, \dots, m_i\}$ where i is the total number of mosaics in M . A mosaic m is composed by four images $m = \{img_1, img_2, img_3, img_4\}$ and characterized by a target class $C(m) = c_{target}$, what the XAI method is expected to explain. While two images of the mosaic belong to the target class $c(img_1) = c(img_2) = c_{target}$, the other two are randomly chosen among the rest of classes $c(img_3) \neq c_{target}; c(img_4) \neq c_{target}$. Mosaics are implemented as two by two grid, with the position of each image being random. Samples of mosaics from different datasets can be seen in Figure 1.

When composing the mosaics we tested two different image configurations: using images of 112x112 pixels (resulting in 224x224 mosaics) and using images of 224x224 pixels (resulting in 448x448 mosaics). For the sake of keeping the same resolution of the visual patterns seen by models during their training, all experiments from §5 use 448x448 mosaics.

3.4 The *Focus* metric

In a sort of eye-tracking game, the *Focus* metric asks to the XAI method “Why does mosaic m belong to class c_{target} ?” on a mosaic m which contains both samples belonging and not belonging to c_{target} . Given the previous question and a good underlying model, any feature attribution method should be able to concentrate most of its explanation relevance on the two appropriated images of the mosaic (i.e., img_1 and img_2 belonging to c_{target}). By explanation relevance we refer to the sum of the positive nonzero values of explanation obtained by a feature attribution method. Thus, the *Focus* metric evaluates the proportion of explanation relevance laying at the appropriated images w.r.t. the total explanation relevance generated for the mosaic. Formally, for a specific mosaic m and target class c_{target} , the *Focus* is defined as:

$$Focus = \frac{R_{img_1} + R_{img_2}}{R_{img_1} + R_{img_2} + R_{img_3} + R_{img_4}} \quad (1)$$

Where R_{img} corresponds to the summed relevance located on the image img . For XAI methods providing both positive and negative relevance (e.g., LRP), only the positive relevance is used.

Assuming a perfectly faithful XAI method X_{perf} , any random model explained by X_{perf} should obtain, on average, a *Focus* of 50%. The main assumption of *Focus* is that, as the model becomes better, this score will grow. Although the theoretical upper-bound of the *Focus* score is 100%, this is unrealistic and undesirable. Such a model would (over)fit the dataset to perfection, have one-hot logits with zero noise, and generalize poorly. Instead, we simply assume an upper-bound close to 100%.

4 Randomization Test

Current evaluations of XAI methods frequently rely on qualitative assessments. These include humans in the loop, thus introducing a significant subjective bias. This is further complicated by the fact that XAI methods are typically designed to focus on prominent, central and/or high contrast areas on the input. When this happens, a XAI method may become more dependant on the input sample than on the underlying model supposedly generating the explanations. To verify that this is not an issue for the *Focus* score, we run randomization tests.

First, we conduct a randomization experiment to assess and decide the exact position of the target class (c_{target}) images within the two by two grid of the mosaic. This experiment uses GradCAM on top of a VGG16 model trained for the

⁴<https://github.com/HPAI-BSC/Focus-Metric>

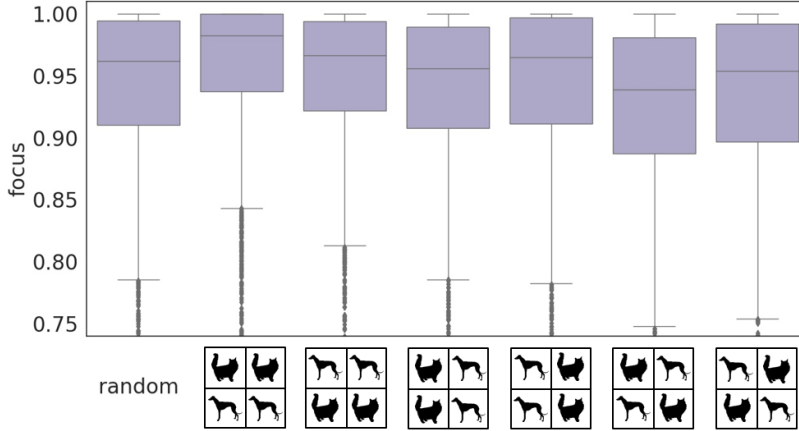


Figure 2: *Focus* obtained by GradCAM on a VGG16 trained for Dogs vs. Cats dataset (pre-trained on ImageNet), using different mosaic configurations. Each box plot shows the distribution of *Focus* obtained from evaluating 2,812 samples for each configuration (the cat being the target).

Dogs vs. Cats dataset (pre-trained on ImageNet). The six possible configurations of the two by two grid were tested, plus a seventh for random positioning. For each configuration 2,812 mosaics were created, using *cat* class as c_{target} . The resulting *Focus* distributions are shown in Figure 2. Clearly, the positioning of target samples has an effect on the *Focus* distribution. Configurations where the two target class images (img_1 and img_2) are arranged contiguously tend to be better, particularly when they are on top. Since we cannot guarantee that these properties will hold among target classes or datasets, we decide to use a sampling approach where the exact position of images is chosen randomly for every mosaic.

The second randomization test aims at evaluating the effect of model randomization on the *Focus* score. For that, we start using two different models. A VGG16 pre-trained on ImageNet and then trained for Dogs vs. Cats, and a totally randomized VGG16 model. The experiment computes the *Focus* metric on the cat target class ($c_{target} = cat$) for the 2,812 mosaics with random layout. The distribution of *Focus* achieved by GradCAM on both models is shown as histograms in Figure 3. While the mean of the *Focus* obtained with the pre-trained model reach a remarkable 0.94, the random model mean score is 0.49, that is roughly 50% of the relevance lays on the wrong class quadrants. To take the randomization analysis beyond, we replicate the experiment of Adebayo *et al.* [2018]. In it, the authors qualitatively pointed at how visual explanations can be compelling to the eye even when randomizing one or more layers of the underlying model. In this experiment, layers are randomized in cascade, starting with only the top layer, and increasingly randomizing more layers one by one until obtaining a fully randomized model. We use GradCAM on InceptionV3 Szegedy *et al.* [2016] (like Adebayo *et al.* [2018]) adding as well VGG16 and ResNet18. Our results are straight-forward: Simply randomizing the top layer (or any other individual or set of layers) makes the *Focus* drop to a 50% mean, the same score obtained by purely random explanations. This illustrates how unbiasing the *Focus* score can be, clearly identifying misleading explanations.

5 Evaluation of XAI methods

In this section we put *Focus* into practice. We evaluate LRP, GradCAM and SmoothGrad using three architectures (VGG16, ResNet18 and AlexNet) and four target datasets (Dogs vs. Cats, ImageNet, MIT67 and MAME). For the Dogs vs. Cats dataset and the MIT67 dataset we use 100 mosaics per target class, a total of 200 and 6,700 mosaics respectively. In the ImageNet experiments a total of 10,000 mosaics are used (10 per target class), while for MAME we use 2,900 mosaics in total (100 per target class).

Figure 4 (a) depicts the *Focus* distributions for the Dogs vs. Cats dataset. Results show a good performance of LRP and GradCAM, reaching a median *Focus* greater than 90%. Notice the three models had a high accuracy for the two-class classification task (as shown in the same figure), as they had been pre-trained with ImageNet. This dataset contains many different breeds of cats and dogs, and pre-training with it guarantees the encoding of a rich set of visual representations within the model. Remarkably, in this experiment, the *Focus* obtained is very similar to the accuracy of the model, with LRP slightly outperforming GradCAM on average.

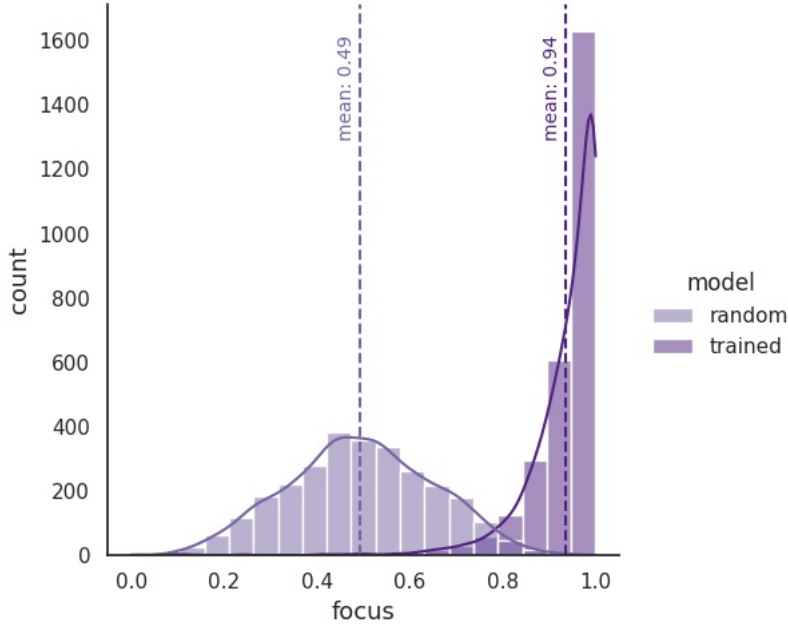


Figure 3: Histogram of *Focus* scores obtained from 2,812 mosaics, using a trained and randomized models. The corresponding PDF estimation is represented by a contour line on top.

On the same experiment, the SmoothGrad method obtains a *Focus* around 50%, that is, totally random. In fact, on all experiments conducted with SmoothGrad the results were similar. This corroborates insights from other studies, which find SmoothGrad analogous to an edge detection method Adebayo et al. [2018], making it a misleading XAI method. Our work provides empirical evidence in that regard.

We further evaluate the three XAI methods using the ImageNet image classification task. We use three pre-trained models, AlexNet⁵, VGG16⁶ and ResNet18⁷, available in the `torchvision.models` subpackage. The main difference between this and the Dogs vs. Cats experiment is the performance of the classifier models. While for the accuracies for Dogs vs. Cats were very high, in ImageNet accuracies are significantly lower, given the complexity of the task. Nonetheless, as shown in Figure 4 (b) LRP still performs competitively, even for AlexNet which only achieves a 36% accuracy at classification. In this case GradCAM shows a slightly superior performance in terms of *Focus* for AlexNet and VGG16. Both LRP and GradCAM manage to obtain higher *Focus* than the corresponding accuracy, while SmoothGrad performs close to randomness.

We also test the XAI methods on the MIT67 dataset, with all models pre-trained on the Places365-Standard dataset Zhou et al. [2017]. Noticeably, these datasets are narrower than ImageNet, containing a smaller variety of target classes. In terms of training samples per class Places365-Standard is close to ImageNet, with 900 and 1,200 correspondingly. In terms of *Focus* distributions, as shown in Figure 4 (c) LRP and GradCAM have a rather different behavior. LRP struggles at focusing on the proper areas of the mosaic for AlexNet, and specially for VGG16. The *Focus* distributions are wider and have a median closer to random behaviour. Since GradCAM also sees its *Focus* diminished, it seems clear that mediocre models generate mediocre explanations. On this same experiment GradCAM performs remarkably well, obtaining *Focus* scores significantly higher than the corresponding model accuracies. Notice GradCAM keeps a narrower distribution, the width of which seems to be aligned with model performance. This alignment occurs in the *Focus* obtained with the GradCAM method in all four experiments (Dogs vs. Cats, ImageNet, MIT67 and MAME): the greater the performance of the model, the smaller the variance of the *Focus* distribution.

Finally, we evaluate the *Focus* distribution for the MAME dataset, as shown in Figure 4 (d). Coherently, SmoothGrad produces random explanations. LRP significantly improves the median and reduces the variance of its *Focus* distribution for ResNet18, while GradCAM is more stable. Further discussion on these outcomes can be found in §7.

⁵<https://download.pytorch.org/models/alexnet-owt-4df8aa71.pth>

⁶<https://download.pytorch.org/models/vgg16-397923af.pth>

⁷<https://download.pytorch.org/models/resnet18-5c106cde.pth>

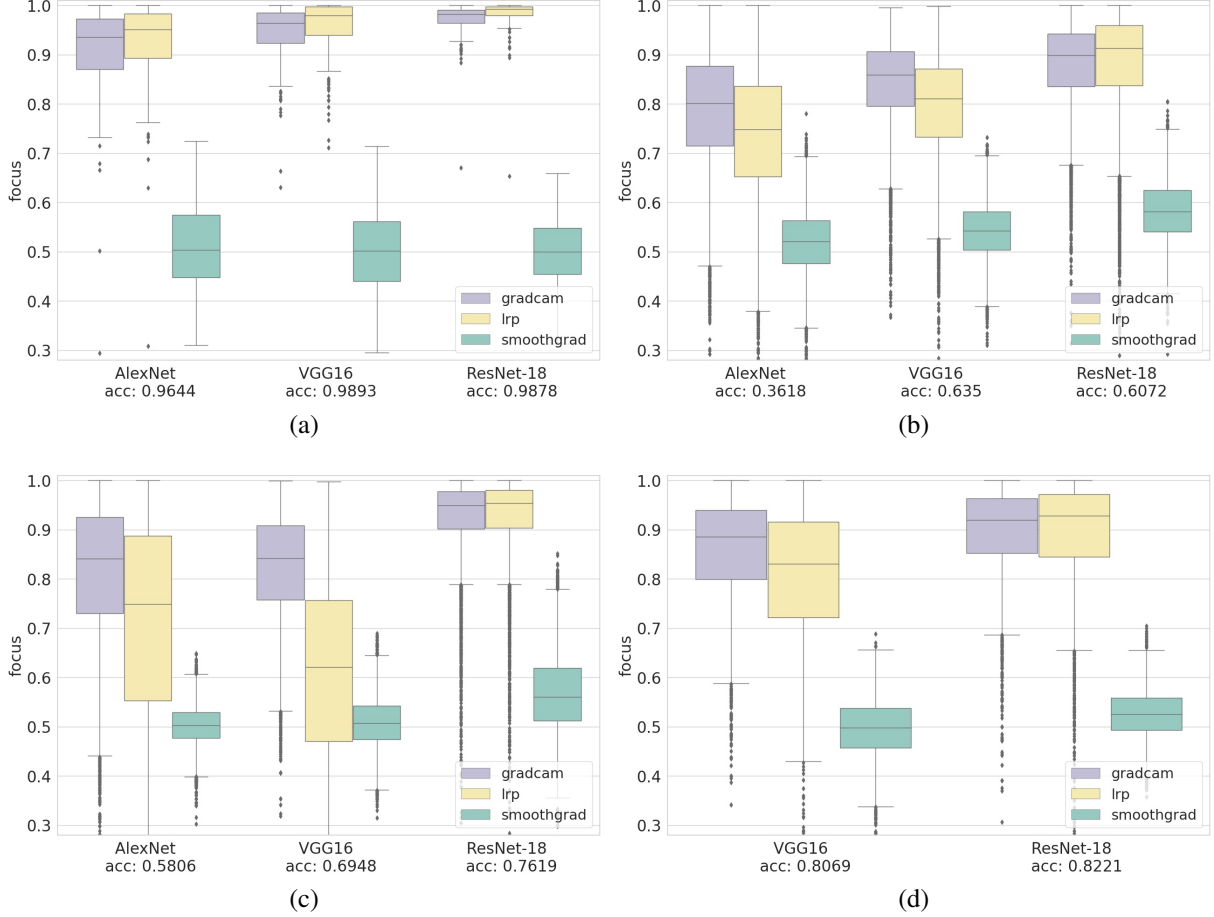


Figure 4: *Focus* distribution obtained by LRP, GradCAM and SmoothGrad on models trained for different datasets. The accuracy (*acc*) shown under each model corresponds to the mean per class accuracy on the validation set of the corresponding dataset. All models were pre-trained on ImageNet, except for MIT67 models which were pre-trained on Places365-Standard. (a) Dogs vs. Cats dataset: distributions correspond to the *Focus* obtained on 200 mosaics (100 per target class). (b) ImageNet dataset: 10,000 mosaics (10 per target class). (c) MIT67 dataset: 6,700 mosaics (100 per target class). (d) MAME dataset: 2,900 mosaics (100 per target class).

6 Discussion

According to the experiments conducted in the previous section, a strong relation exists between the model performance and the *Focus* score. To further validate such correlation, we evaluate the evolution of the *Focus* metric and its corresponding accuracy during a model training process. In particular, we extract *Focus* after every training epoch, plotting the median of the corresponding distribution. The *Focus* metric is evaluated using the most stable explainability method according to our results, the GradCAM method. Regarding the model, it uses the ResNet18 architecture trained with Dogs vs. Cats dataset, the combination providing best performance results. This experiment is performed under two different setups: training from scratch and training on top of an ImageNet pre-trained model. Results of this experiment are shown in Figure 5, illustrating a clear correlation between *Focus* and model performance. For the training from a pre-trained model (top plot), the Pearson correlation coefficient is 0.9939 and, for the training from scratch case (bottom plot), the Pearson correlation coefficient is 0.9873. Additionally, notice the *Focus* metric reduces its variance while the training of the model converges (shown as a shaded area around *Focus* score).

Beyond the relation between *Focus* and model performance, there are other factors affecting the *Focus* outcome. Among the ones we consider are architectures and datasets (having fixed GradCAM as the XAI method). To assess their impact, we look at all the experiments conducted in §5, plotting their median *Focus* scores *w.r.t.* model performance in two plots (Figure 6): one plotting *Focus* versus accuracy (a) and another plotting *Focus* versus loss (b).

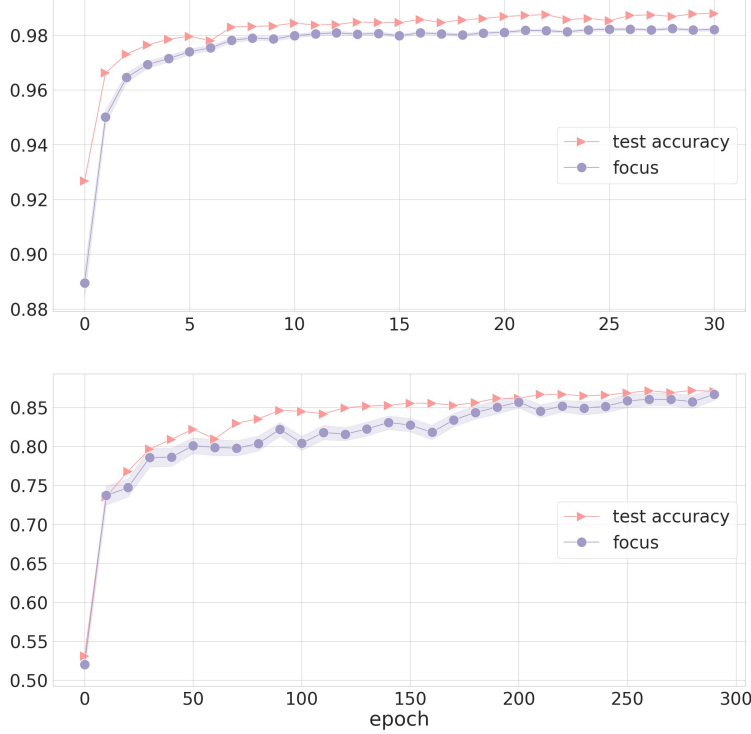


Figure 5: Model’s training curves as pink triangles, median of the *Focus* distribution in purple (variance as shaded area). Both curves correspond to a ResNet18 trained on the Dogs vs. Cats dataset. Top plot corresponds to a model pre-trained on ImageNet, while the bottom plot corresponds to a model trained from scratch.

Let us first discuss model architecture. While performance and *Focus* score are strongly correlated, there are cases where a better performance does not entail a better *Focus*. Three of our experiments show or approximate such scenario, always when switching from VGG16 to ResNet18 architecture while using the same dataset. For the MAMe dataset (pink and grey circles), performance slightly increases when moving from VGG16 to ResNet18 (+1.52%) while *Focus* grows considerably (+3.39%). For the Dogs vs. Cats dataset (pink and grey stars), performance remains roughly equal (-0.15%) while *Focus* increases (+1.77%). Finally, the most remarkable case is for the ImageNet dataset (pink and grey squares), where performance degrades (-2.78%) while the *Focus* significantly improves (+4.03%). According to these results, when switching from VGG16 to ResNet18 we can expect an improvement in *Focus*, even when such models are equally good at the underlying task. This particular experiment showcases the relevance of architecture for the *Focus*, and potentially for XAI. That being said, further experimentation needs to be conducted with a wider variety of designs.

The other main factor influencing the *Focus* score according to our experiments is the target task (*i.e.*, the dataset). There are two cases where having the same architecture but different dataset, model performance degrades while *Focus* improves, showing the effect of the dataset itself. The first example is for ResNet18 trained for either MAMe or MIT67 (grey circle and grey triangle). While for the MIT67 accuracy is worse (-6.02% acc), the same model outperforms the MAMe one in terms of *Focus* (+2.98%). The second case involves VGG16 models trained for MIT67 and ImageNet (pink triangle and pink square), where, when comparing both models, the latter’s accuracy degrades by a -6.98% while its *Focus* score improves a +1.71%. These results illustrate the impact of dataset on the *Focus* score. Several factors may be at play here, including number of classes in the task, how fine-grained or varied these are, the pre-training used, and the training set size.

7 Conclusion

With the aim of evaluating XAI methods in a quantitative manner, we introduce a novel metric that approximates how faithful an explanation is to the behavior of the underlying model. We show the methodology to be consistent and resilient to misleading explanations.

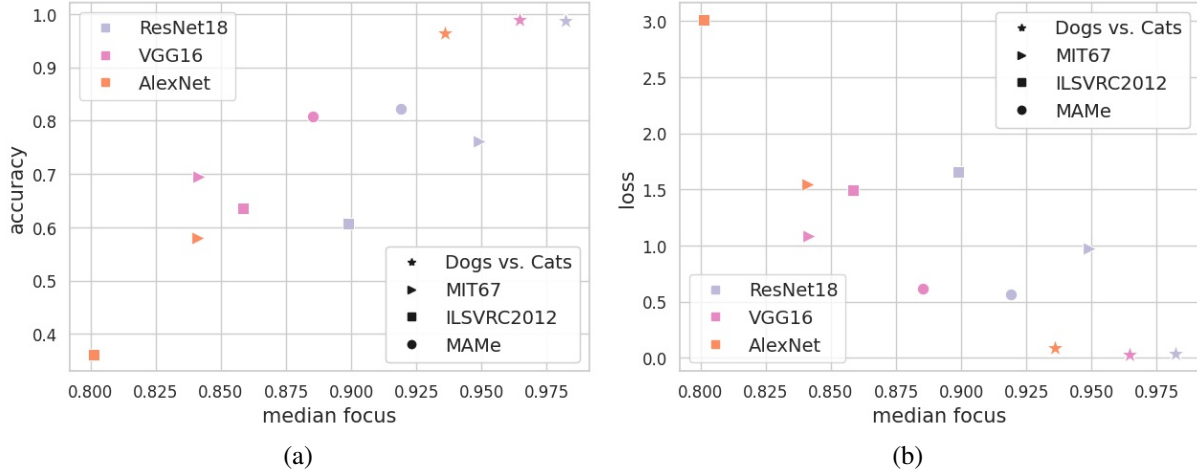


Figure 6: Model accuracy (a) and model loss (b) vs median of the *Focus* distribution for different experiments. Each architecture is shown in a different color and each classification task is represented with a different marker.

When applied to SmoothGrad, the *Focus* score labels the methodology as quasi-random in its explanations *w.r.t.* the model. On the contrary, LRP and GradCAM are both found to be reliable methodologies for XAI in terms of faithfulness: In general, better models yield more accurate explanations.

According to the *Focus* score, LRP performs much better when a powerful pre-training is performed and/or when the model has very high accuracy at the task. On the other hand, GradCAM performs consistently well, remarkably so even when the underlying model performs poorly at the task, but scores a bit lower than LRP on very high accuracy models. One hypothesis for this behavior is the limited precision of GradCAM. While LRP produces pixel level, crisp explanations, GradCAM generates blurry patches that easily overflow the explanation target into neighbouring images of the non-target class (see Figure 1 for example). Such lack of preciseness is penalized by *Focus* which detects the overflow of explanation leaking over. With regards to architectures, our experiments show a clear superiority of ResNet18 over VGG16 and AlexNet when generating explanations.

We found a strong positive correlation between model performance and *Focus* score, a relation that is also affected by other factors. These include model architecture and target task/dataset, resulting in cases where a better performance does not yield a better *Focus*. This finding speaks of the importance of assessing models by other means than just task performance optimization (*e.g.*, *accuracy*), and opens the door to the selection of models also by taking into account the quality of its explanations (*e.g.*, *Focus*). Finally, we hope that the *Focus* will serve to move towards a standardization of the evaluation metrics in the field of XAI methods.

Acknowledgements

This work is supported by the European Union – Horizon 2020 Program under the scheme “INFRAIA-01-2018-2019 – Integrating Activities for Advanced Communities”, Grant Agreement n.871042, “SoBigData++: European Integrated Infrastructure for Social Mining and Big Data Analytics” (<http://www.sobigdata.eu>) and by the Departament de Recerca i Universitats of the Generalitat de Catalunya under the Industrial Doctorate Grant DI 2018-100.

References

- Leilani H Gilpin, David Bau, Ben Z Yuan, Ayesha Bajwa, Michael Specter, and Lalana Kagal. Explaining explanations: An overview of interpretability of machine learning. In *2018 IEEE 5th International Conference on data science and advanced analytics (DSAA)*, pages 80–89. IEEE, 2018.
- Sina Mohseni, Niloofar Zarei, and Eric D Ragan. A multidisciplinary survey and framework for design and evaluation of explainable ai systems. *arXiv preprint arXiv:1811.11839*, 2018.
- Ramprasaath R. Selvaraju, Michael Cogswell, Abhishek Das, Ramakrishna Vedantam, Devi Parikh, and Dhruv Batra. Grad-cam: Visual explanations from deep networks via gradient-based localization. *International Journal*

- of Computer Vision*, 128(2):336–359, Oct 2019. ISSN 1573-1405. doi:10.1007/s11263-019-01228-7. URL <http://dx.doi.org/10.1007/s11263-019-01228-7>.
- Karen Simonyan, Andrea Vedaldi, and Andrew Zisserman. Deep inside convolutional networks: Visualising image classification models and saliency maps. In *In Workshop at International Conference on Learning Representations*. Citeseer, 2014.
- Daniel Smilkov, Nikhil Thorat, Been Kim, Fernanda Viégas, and Martin Wattenberg. Smoothgrad: removing noise by adding noise. *arXiv preprint arXiv:1706.03825*, 2017.
- Sebastian Bach, Alexander Binder, Grégoire Montavon, Frederick Klauschen, Klaus-Robert Müller, and Wojciech Samek. On pixel-wise explanations for non-linear classifier decisions by layer-wise relevance propagation. *PloS one*, 10(7):e0130140, 2015.
- Julius Adebayo, Justin Gilmer, Michael Muelly, Ian Goodfellow, Moritz Hardt, and Been Kim. Sanity checks for saliency maps. *arXiv preprint arXiv:1810.03292*, 2018.
- Mukund Sundararajan, Ankur Taly, and Qiqi Yan. Axiomatic attribution for deep networks. In *International Conference on Machine Learning*, pages 3319–3328. PMLR, 2017.
- Jianming Zhang, Sarah Adel Bargal, Zhe Lin, Jonathan Brandt, Xiaohui Shen, and Stan Sclaroff. Top-down neural attention by excitation backprop. *International Journal of Computer Vision*, 126(10):1084–1102, 2018.
- Wojciech Samek and Klaus-Robert Müller. Towards explainable artificial intelligence. In *Explainable AI: interpreting, explaining and visualizing deep learning*, pages 5–22. Springer, 2019.
- Wojciech Samek, Alexander Binder, Grégoire Montavon, Sebastian Lapuschkin, and Klaus-Robert Müller. Evaluating the visualization of what a deep neural network has learned. *IEEE transactions on neural networks and learning systems*, 28(11):2660–2673, 2016.
- Woo-Jeoung Nam, Shir Gur, Jaesik Choi, Lior Wolf, and Seong-Whan Lee. Relative attributing propagation: Interpreting the comparative contributions of individual units in deep neural networks, 2019.
- Grégoire Montavon, Sebastian Lapuschkin, Alexander Binder, Wojciech Samek, and Klaus-Robert Müller. Explaining nonlinear classification decisions with deep taylor decomposition. *Pattern Recognition*, 65:211–222, 2017.
- Alex Krizhevsky, Ilya Sutskever, and Geoffrey E Hinton. Imagenet classification with deep convolutional neural networks. *Advances in neural information processing systems*, 25:1097–1105, 2012.
- Karen Simonyan and Andrew Zisserman. Very deep convolutional networks for large-scale image recognition. *arXiv preprint arXiv:1409.1556*, 2014.
- Kaiming He, Xiangyu Zhang, Shaoqing Ren, and Jian Sun. Deep residual learning for image recognition. In *Proceedings of the IEEE conference on computer vision and pattern recognition*, pages 770–778, 2016.
- Olga Russakovsky, Jia Deng, Hao Su, Jonathan Krause, Sanjeev Satheesh, Sean Ma, Zhiheng Huang, Andrej Karpathy, Aditya Khosla, Michael Bernstein, et al. Imagenet large scale visual recognition challenge. *International journal of computer vision*, 115(3):211–252, 2015.
- Ariadna Quattoni and Antonio Torralba. Recognizing indoor scenes. In *2009 IEEE Conference on Computer Vision and Pattern Recognition*, pages 413–420. IEEE, 2009.
- Ferran Parés, Anna Arias-Duart, Dario Garcia-Gasulla, Gema Campo-Francés, Nina Viladrich, Eduard Ayguadé, and Jesús Labarta. The mame dataset: On the relevance of high resolution and variable shape image properties, 2021.
- Sashank J Reddi, Satyen Kale, and Sanjiv Kumar. On the convergence of adam and beyond. *arXiv preprint arXiv:1904.09237*, 2019.
- Christian Szegedy, Vincent Vanhoucke, Sergey Ioffe, Jon Shlens, and Zbigniew Wojna. Rethinking the inception architecture for computer vision. In *Proceedings of the IEEE conference on computer vision and pattern recognition*, pages 2818–2826, 2016.
- Bolei Zhou, Agata Lapedriza, Aditya Khosla, Aude Oliva, and Antonio Torralba. Places: A 10 million image database for scene recognition. *IEEE Transactions on Pattern Analysis and Machine Intelligence*, 2017.